Energy Equip. Sys./ Vol. 5/No.4/December 2017/ 325-339

ENERGY EQUIPSYS

Energy Equipment and Systems

http://energyequipsys.ut.ac.ir
www.energyequipsys.com

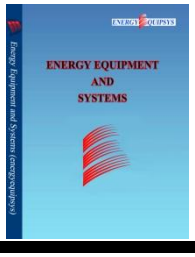

Selection of the optimum prime mover and the working fluid in a regenerative organic rankine cycle

Authors

Hassan Hajabdollahi [a*]
Alireza Esmaieli [a]

[a] Department of Mechanical Engineering, Vali-e-Asr University of Rafsanjan, Rafsanjan, Iran

ABSTRACT

A regenerative organic Rankine cycle (RORC) is modeled and optimized for the use of waste heat recovery from a prime mover (PM). Three PMs including, a diesel engine, a gas engine, and a microturbine are selected in this study. Four refrigerants including isobutane, R123, R134a, and R245fa are selected. The nominal capacity of the PM, PM operating partial load, turbine inlet pressure, condenser pressure, refrigerant mass flow rate, pump efficiency, turbine efficiency, and regenerator effectiveness are considered as the decision variables. Then, the Genetic Algorithm is applied to maximize the thermal efficiency and minimize the total annual cost (TAC), simultaneously. The optimum results demonstrate that the best working fluid and the PM are, respectively, R123 and the diesel engine, which have a thermal efficiency of 0.50 and a TAC of $170,276/year. The optimum results are compared with each of the other studied cases. For example, the optimum result in the case of a diesel engine working with R123 shows a 2% and 2.52% improvement in the thermal efficiency and the TAC, respectively, in comparison to the case of a gas engine working with R123. Furthermore, a 26% and an 18.38% improvement in the thermal efficiency and the TAC are found when the best-studied cycle is compared with a microturbine and R123.

Article history:

Received : 13 October 2016
Accepted : 19 September 2017

Keywords: Regenerative Organic Rankine Cycle, Prime Mover, Total Annual Cost, Thermal Efficiency, Working Fluid.

1. Introduction

In recent years, noticeable investigations in the field of organic Rankine cycles (ORC) have been performed due to the ability of working with low-temperature heat sources. The organic Rankine cycle with a regenerator has a higher efficiency in comparison with the simple organic Rankine cycle. Mago and Carcasci et al. investigated the effect of different working fluids on the organic Rankine cycle for low-grade waste heat recovery [1–2]. Yun et al. simulated a dual parallel organic Rankine cycle (ORC) system for high efficiency waste heat recovery in marine applications and the results indicated that the performance of a dual ORC to generate more total power output is better than the single ORC [3]. Gong et al. presented the thermodynamic performance analysis of a coupled transcritical and subcritical organic Rankine cycle (CORC) system for waste heat recovery. The results showed that an increase

*Corresponding author: Hassan Hajabdollahi
Address: Assistant Professor, Department of Mechanical Engineering, Vali-e-Asr University of Rafsanjan, Kerman, Iran
E-mail address: H.Hajabdollahi@vru.ac.ir

of the pinch point temperature difference of the internal heat exchanger decreased the net power output and the thermal efficiency of the CORC [4]. Coskun et al. performed a thermodynamic analysis and optimization of various power cycles for a geothermal resource [5]. Li et al. proposed the performance of the ORC systems and used zeotropic mixtures as working fluids in order to recover the waste heat of flue gas from an industrial boiler based on thermodynamics and thermo-economics under different operating conditions. The results showed that the mixture of working fluids had an important effect on the ORC system efficiency, which is related to the temperature glide during the changing of phase in the mixtures [6]. Certain authors optimized the regenerative organic Rankine cycle and the organic Rankine cycle for waste heat recovery from the thermo-economic or environmental viewpoint [7–11]. Yang and Yeh used six working fluids for an organic Rankine cycle with zero ozone depletion potential and low global warming potential in order to recover waste heat from cylinder jackets of water from large marine diesel engines [12]. In other research, Feidt et al. proposed the system efficiency optimization scenarios of basic and regenerative supercritical ORCs using low-GWP (global warming potential) organic compounds as working fluids [13]. Yang and Yeh described the thermodynamic and economic performance optimization for an ORC system and compared it to an ORC system with a pre-heater. They found that the payback periods of the ORC system were higher than an ORC system with a pre-heater [14]. Feng et al. used a multiobjective optimization technique to maximize the exergy efficiency and the net power output as well as to minimize the levelized energy cost between a regenerative organic Rankine cycle (RORC) and a basic organic Rankine cycle (BORC). They found an 8.1% improvement in exergy efficiency in the case of the RORC in comparison with the BORC [15]. A number of researchers presented a thermodynamic analysis and optimization of a solar organic Rankine cycle system using various working fluids [16–18]. Hajabdollahi et al. optimized a regenerative solar organic Rankine cycle with various working fluids by considering an hourly analysis and applied the real-parameter genetic algorithm (RPGA). Their results revealed that the best-studied working fluid is isobutane from an economic viewpoint; this is followed by R245fa and R123 [19]. Imran et al. and Walraven et al. optimized an evaporator and air-cooled organic Rankine cycle for a low-temperature geothermal heat source [20–21]. The present study deals with the development of a hydraulic and a thermal design model of a chevron-type plate evaporator and the optimization of its geometrical parameters for a low temperature geothermal ORC system.

In this paper, after the thermo-economic and environment modeling of RORC (regenerative organic Rankine cycle) for waste heat recovery from the PM, the optimization is performed to maximize the thermal efficiency and minimize the total annual cost, simultaneously. The nominal capacity of the PM, the PM-operating partial load, the turbine inlet pressure, the condenser pressure, the refrigerant mass flow rate, the turbine isentropic efficiency, the pump isentropic efficiency, and the regenerator effectiveness are considered as the eight decision variables. Then, the NSGA-II technique is used to provide a set of optimum results. In summary, the following items are the goals of this paper:

- Perform four simultaneous analyses, including the categories of efficiency, energy, economic, and environment, which provide a 4E analysis for equipment selection.
- Choice of nominal capacity of PM, PM-operating partial load, turbine inlet pressure, condenser pressure, turbine isentropic efficiency, refrigerant mass flow rate, pump isentropic efficiency, and regenerator effectiveness as design variables.
- Perform multiobjective optimization by considering the efficiency and the total annual cost as the two fitness functions.
- Perform the optimization for four working fluids including isobutane, R123, R134a, and R245fa using a diesel engine, gas engine, and microturbine as the three prime movers.
- Finally, perform a sensitivity analysis on the total annual cost by increasing the fuel and the cycle equipment price.

Nomenclature

A	Heat transfer surface area (m^2)
C	Cost ($/year)
E_{nom}	Nominal capacity of prime mover (kW)
h	Enthalpy (kJ/kg K)
inf	Interest rate (–)
LHV	Fuel lower heating value (kJ/kg)
$\dot{m}$	Mass flow rate (kg/s)
PL	Partial load (%)

$\dot{Q}$ Rate of heat transfer (kW)
T Temperature (°C)
U Overall heat transfer coefficient (W/m^2.K)
$\dot{W}$ Power (kW)
x Working fluid quality (–)
y Depreciation time (year)

Greek abbreviation

α Annual cost coefficient (–)
ε Total cycle thermal efficiency (–)
η Efficiency (–)
κ Effectiveness (–)
υ Specific volume (m^3/kg)
ρ Density (kg/m^3)
τ Hours of operation per year (hour)
φ Maintenance factor (–)
ψ_{em} Pollutant emission cost ($/kg)
ψ_f Fuel cost ($/kg)

Subscripts

a Actual
amb Ambient
cond Condenser
CW Cooling water
DE Diesel engine
env Environment
evap Evaporator
f Fuel
GE Gas engine
i Inlet
inv Investment
LMTD Logarithmic mean temperature difference
M Microturbine
nom Nominal
o Outlet
RORC Regenerative Organic Rankine Cycle
PM Prime Mover
Pump Pump
R Regenerator
s Isentropic
T Turbine
stack Stack
total Total

2. Thermal modeling

The system considered in this work consists of a PM (diesel engine or gas engine or microturbine) as well as a Rankine cycle including a turbine, condenser, evaporator, pump, and regenerator. A schematic diagram is shown in Fig. 1.

The recovered heat from the PM increases the refrigerant temperature in the evaporator (State 7). The refrigerant outlet of the evaporator is superheated (State 1) and by passing through the expander (turbine), it loses some of its energy and with a relatively high quality, it enters the regenerator (State 2) and leaves the regenerator with the loss of some energy. The refrigerant enters the condenser (State 3), transfers heat to the cooling tower, and then condenses. Then, the pressure of the liquid increases in the pump (State 4). The working fluid is preheated in the regenerator (State 5) and then enters the evaporator (State 6). The net power of the PM and the Rankine cycle are the sources of power generation in this system. In order to perform thermal modeling, the mass and the energy balances on the system are presented to determine the flow rates and the energy transfer rates at control volumes. By applying the first law of thermodynamic in the steady state, one can find the formula for the mass and energy balance as follows [22]:

Mass balance equation:

$$\sum \dot{m}_i = \sum \dot{m}_o \quad (1)$$

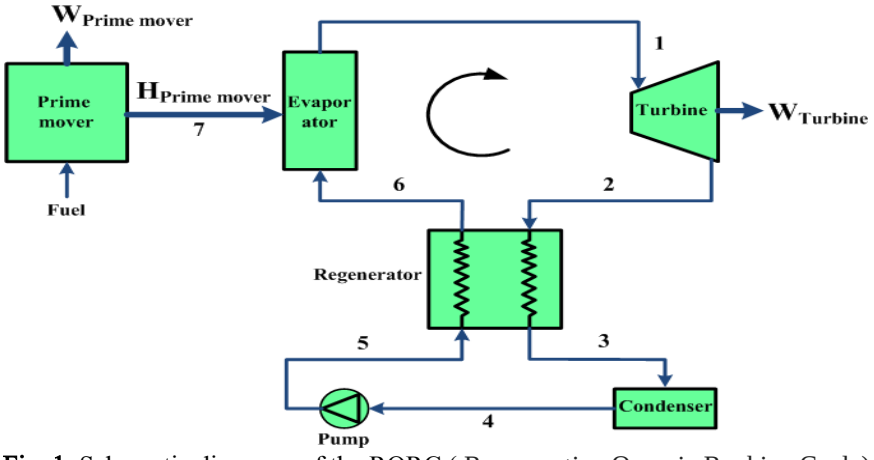

Fig. 1. Schematic diagrams of the RORC (Regenerative Organic Rankine Cycle)

Energy balance equation:

$$\dot{Q} - \dot{W} = \sum \dot{m}_o h_o - \sum \dot{m}_i h_i \quad (2)$$

where i and o are the inlet and the outlet of flow in the control volume.

The energy balance equations for the cycle components are as follows:

Turbine:

$$\eta_T = \frac{\dot{W}_{T,a}}{\dot{W}_{T,s}} = \frac{h_i - h_{o,a}}{h_i - h_{o,s}} \quad (3)$$

$$\dot{W}_{T,a} = \sum \dot{m}_i h_i - \sum \dot{m}_o h_o \quad (4)$$

Regenerator:

$$\kappa_R = \frac{h_6 - h_5}{h_2 - h_5} \quad (5)$$

$$A_R = \frac{\dot{m}(h_2 - h_3)}{0.1 LMTD_R} \quad (6)$$

$$LMTD_R = T_2 - T_6 \quad (7)$$

Here, κ_R, A_R, and $LMTD_R$ are the regenerator effectiveness, the regenerator heat transfer surface area, and the regenerator logarithmic mean temperature difference.

Condenser:

$$\dot{Q}_{cond} = \sum \dot{m}_i h_i - \sum \dot{m}_o h_o = U A_{cond} \Delta T_{LMTD} \quad (8)$$

The A_{cond} and ΔT_{LMTD} are the condenser heat transfer surface area and the logarithmic mean temperature difference, which are defined as follows:

$$A_{cond} = \frac{\dot{Q}_{PM}}{F \times U \times LMTD_{cond}} \quad (9)$$

$$LMTD_{cond} = \frac{(T_3 - 25) - (T_4 - 15)}{log\left(\frac{T_3 - 25}{T_4 - 15}\right)} \quad (10)$$

$$\Delta T_{LMTD} = \frac{\Delta T_1 - \Delta T_2}{log(\Delta T_1 / \Delta T_2)} = \frac{(T_2 - T_{CW,o}) - (T_3 - T_{CW,i})}{log\left((T_2 - T_{CW,o}) / (T_3 - T_{CW,i})\right)} \quad (11)$$

where Q_{PM} is the useful heat of the PM ($\dot{Q}_{PM}$ has been obtained using the curve fitted data available in [23]) and is listed as a function of the partial load in Appendix A. $LMTD_{cond}$ is the condenser logarithmic mean temperature difference and CW indicates the cooling water recirculation in the condenser. The pressure drop in the condenser, evaporator, and regenerator are defined as follows:

$$\Delta p = \left(1 - \frac{p_o}{p_i}\right) \quad (12)$$

Pump:

$$\eta_{Pump} = \frac{\dot{W}_{Pump,s}}{\dot{W}_{Pump,a}} = \frac{\upsilon_i (P_o - P_i)}{h_o - h_i} \quad (13)$$

Evaporator:

$$\dot{Q}_{evap} = \dot{m}_i (h_o - h_i) \quad (14)$$

Prime mover:

A part of the input energy to the prime movers is converted to power, which is a function of the partial load and is estimated with the relations listed in Appendix B. With an increase in partial load, the power, the recoverable heat rate, and the fuel mass flow rate are also increased [10]. The fuel mass flow rate relations of the prime movers at different partial loads are listed in Appendix C. Here, $\dot{m}_{f,nom}$ is the nominal prime mover fuel consumption computed as follows:

$$\dot{m}_{f,nom} = \frac{E_{nom,PM}}{LHV_f \, \eta_{nom}} \quad (15)$$

where $E_{nom, PM,}$ and η_{nom} are the nominal capacity and the nominal efficiency of the PM. The nominal efficiency of different studied PMs is approximated with the relations listed in Appendix D.

Total cycle:

Net power generated in the RORC is obtained as shown below:

$$\dot{W}_{RORC} = \dot{W}_{T,a} - \dot{W}_{Pump,a} \quad (16)$$

And, finally, the total thermal efficiency of the entire system is calculated as follows:

$$\varepsilon = \frac{\dot{W}_{total}}{\dot{m}_f . LHV_f} \quad (17)$$

where $\dot{W}_{total}$ is the total output net power of the system and is approximated as follows:

$$\dot{W}_{total} = \dot{W}_{PM} + \dot{W}_{RORC} \quad (18)$$

3. Objective functions and constraints

In this work, the thermal efficiency and the total annual cost of the system are considered as the two fitness functions. The efficiency defined in Eq. (17) and the total annual cost includes investment cost, the cost of PM fuel as well as the environmental cost, which are estimated as follows:

$$C_{total} = \alpha\varphi C_{inv} + C_f + C_{env} \quad (19)$$

Here, C_{inv} is the purchase cost of the components and is listed in Appendix E. It is worth mentioning that the evaporator is a part of the prime mover and is included in the cost of the PM. Moreover, α is the annual cost coefficient that is defined as follows:

$$\alpha = \frac{inf}{1-(1+inf)^{-y}} \quad (20)$$

where inf and y represent the interest rate and the depreciation time. The total cost of equipment, including PM, turbine, pump, and condenser as well as the regenerator is obtained as follows:

$$C_{inv} = C_{inv,PM} + C_{inv,T} + C_{inv,Pump} + C_{inv,cond} + C_{inv,R} \quad (21)$$

The fuel and environmental costs that are defined in Eq. (19) are computed from the following equations:

$$C_{f,DE} = \frac{d_1 \dot{m}_{f,DE} \psi_{f,DE} \tau}{\rho_{f,DE}} \quad (22)$$

$$C_{f,GE/M} = \frac{d_2 \dot{m}_{f,GE/M} \psi_{f,GE/M} \tau}{\rho_{f,GE/M}} \quad (23)$$

$$C_{env,DE} = d_3 \times \psi_{em} \times \tau \times \dot{m}_{f,DE} \quad (24)$$

$$C_{env,GE/M} = d_4 \times \psi_{em} \times \tau \times \dot{m}_{f,GE/M} \quad (25)$$

Here, ψ_{em}, τ and $\dot{m}_{f,GE/M}$ are the unit price of emissions, the number of hours of operation per year, and the fuel consumption rate of the gas engine or the microturbine, respectively. The constant value of the d coefficients is estimated using the curve fitted data available in Eq. [23]. The system has been limited by constraints that are introduced as follows:

$$P_1 > P_2 \quad (26)$$

$$W_{total} > W_{req} \quad (27)$$

where W_{req} is the required power dependent on each case study.

$$T_3 > 40℃ \quad (28)$$

The above constraints are used for the keeping the condenser temperature above the ambient temperature for the condensing trend.

$$x_2 > 0.95 \quad (29)$$

This constraint is applied to prevent turbine end blade corrosion. Furthermore, in order to avoid PM stack corrosion, the stack temperature is assumed to be above 148.8 ℃ and 250℃ for the diesel and gas engine, and the microturbine, respectively [23].

4. Genetic algorithm for multiobjective optimization

In this study, the fast and the elitist nondominated sorting genetic algorithm (NSGA-II) is proposed as an optimization algorithm. The steps of this algorithm are briefly described as follows [24–25]:

The initial population is generated in such way that it is a single objective genetic algorithm. After population coding and function evaluation, the population is sorted based on nondomination sorting and forms as fronts [25]. The first ranked front is a completely nondominant set in the current population, and the second front is only dominated by the individuals in the first front and the front continues as such. Each individual is assigned rank values or based on the front to which they belong in each front. The fitness values of individuals are selected (1) in the first front, and for the second, they are assigned to be (2), and so on. In addition to the fitness value, a new parameter is also calculated for each individual, which is called the crowding distance [25]. The crowding distance demonstrates how close a point is to its neighbors. It should be mentioned that the large average crowding distance would be produced with better diversity in the population. In this method, a binary tournament selection is used to select parents from the population according to the rank and the crowding distance. An individual selected in the rank is lesser than the others or if crowding distance is greater than the others. Offspring are generated by the selected population from mutation and crossover operators as well as by choosing the number of individuals from each subpopulation, where the influence of elitism is controlled in order to preserve diversity [26].

The new population is sorted once again according to nondomination and only the best N individuals are selected, where N is the population size. The selection is made on the basis of the rank and the crowding distance on the last front.

5. Case study

In the present case study, a plant with a net output power of 300 kW is required. The optimization was performed for a depreciation time of y = 20 years, τ = 6000 hours in a year, interest rate inf = 0.12, and the cost of carbon dioxide emissions ψ_{em} = \$0.02086 /kg [10]. To optimize the plant, four working fluids including isobutane, R123, R245fa, and R134a were selected. In addition, optimization was performed for three different PMs, a diesel engine, a gas engine, and a microturbine, separately. The nominal capacity of the PM, PM-operating partial load, turbine inlet pressure, condenser pressure, refrigerant mass flow rate, turbine isentropic efficiency, pump isentropic efficiency, and regenerator effectiveness were considered as the decision variables to minimize the total annual cost and maximize the efficiency. The higher and lower range of the decision variables are listed in Table 1. It should be noted that the zero for the lower range of regenerator effectiveness indicates a plant without a regenerator. The diesel fuel cost and the gas fuel cost were ψ_f = 0.144 \$/kg and ψ_f = 0.125 \$/kg, respectively [28]. In this system, φ = 1.05 and Δp = 3% were assumed for the maintenance factor and the pressure drop in the evaporator, condenser, and regenerator, and the constants of the relations of Eqs. (22–25) are taken as d = [1200 1.2 10980 9900].

6. Results and discussion

6.1. Trend of thermo–economic and environment analysis

In this work, the ORC with a regenerator simulation program is written in MATLAB and the simulation procedure is indicated in Fig. 2. The heat and the produced power from the prime mover (PM) depends on the nominal capacity of the PM and its partial load using the relations listed in Appendices A and B. The investment cost of equipment, considering the nominal capacity of PM, turbine inlet pressure, turbine isentropic efficiency, turbine inlet temperature, pump isentropic efficiency, pump outlet pressure, and condenser as well as regenerator heat transfer surface area are computed from the relations listed in Appendix E. Taking into account the investment cost of equipment, fuel, pollution, power generation, and net power output from the RORC, the total annual cost (TAC) and total cycle thermal efficiency are computed by Eqss (19) and (17), respectively.

6.2. Optimization

To find the optimum Pareto fronts in each case, NSGA-II is used for 2,500 generations, with a search population size of M = 400 individuals, a gene mutation probability of p_m = 0.035, a crossover probability of p_c = 0.9, and a controlled elitism value of c = 0.55. To increase the performance of calculations in the developed code, seven simultaneous programs are run on a system with an i7-3200GHz core processor. The optimum Pareto fronts for different studied PMs and working fluids are shown in Figs. 3 and 4. It should be noted that to have a good Pareto front with high diversity and enough nondominated points, each program was run three times and all the obtained Pareto fronts were ranked again, and the first ranked Pareto is selected as the final optimum Pareto front. The Pareto-optimal fronts for the different studied refrigerants in the specific PM are illustrated in Fig. 3. As depicted in Fig. 3,

Table.1. The design parameters, their range of variation and their change step

Variables	From	To	Change step
Nominal capacity of prime mover (kW)	10	300	0.001
Prime mover operating partial load (kW)	50	100	0.001
Turbine inlet pressure (kPa)	100	2000	0.001
Condenser pressure (kPa)	50	2000	0.001
refrigerant mass flow rate (kg/s)	0.1	10	0.001
Turbine isentropic efficiency (-)	0.5	0.9	0.001
Pump isentropic efficiency (-)	0.5	0.9	0.001
Regenerator effectiveness (-)	0	0.9	0.001

the best-studied working fluid is R123. In fact, Pareto fronts in the case of R123 by having the maximum efficiency of 0.51, 0.50 and 0.39 as well as a minimum TAC of $165,970/year, $169,660/year, and $195,330/year, respectively, for diesel engine, gas engine, and microturbine, dominated the other fronts. Actually, the T-S diagram of R123 has a lower and positive slope in comparison to the other studied refrigerants, which increased the temperature and the enthalpy difference (turbine power) for a specific value of pressure differences [29]. The refrigerants R245fa, isobutene, and R134a are, respectively, the next in line in terms of ranking.

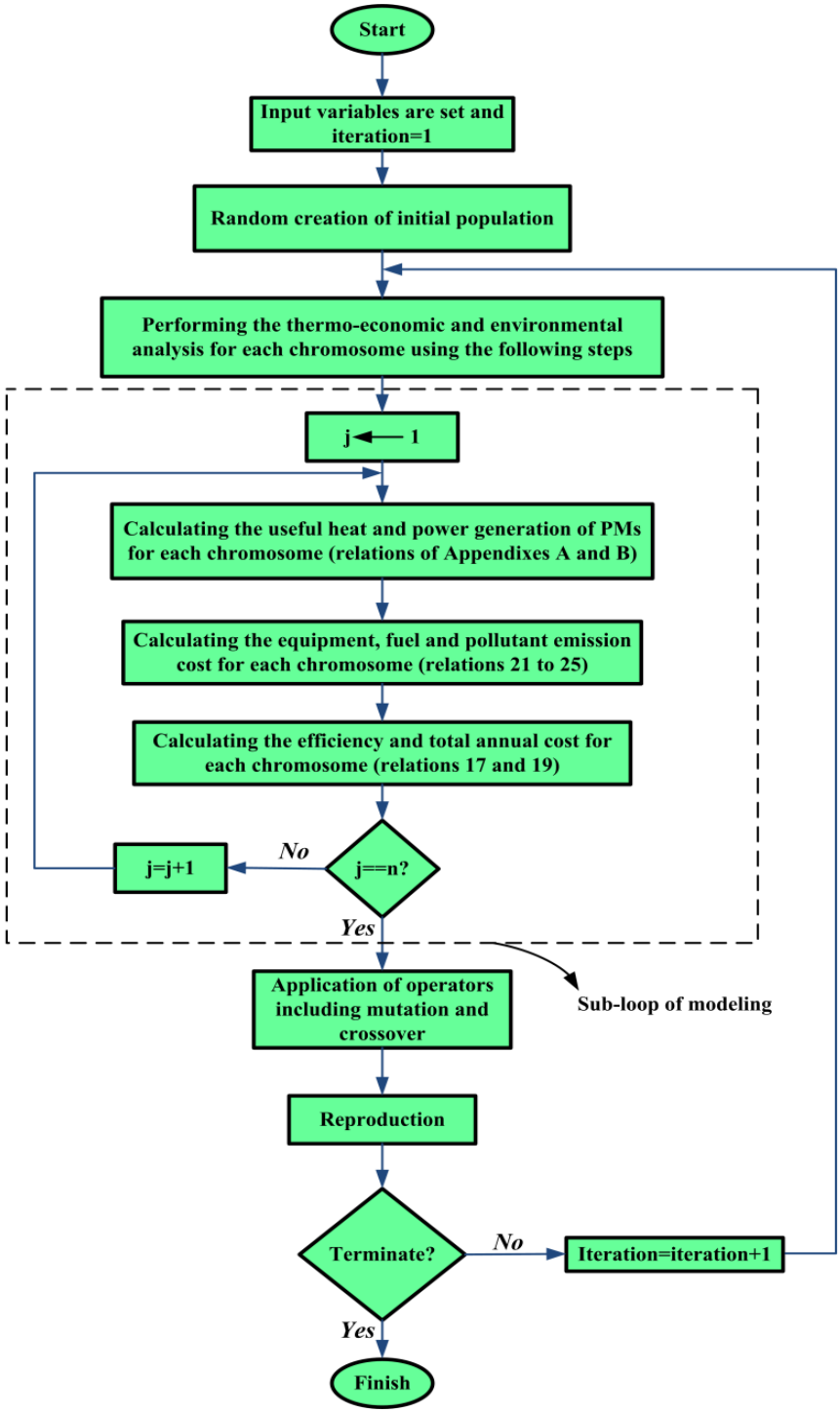

Fig. 2. The simulation flowchart of the RORC (Regenerative Organic Rankine Cycle)

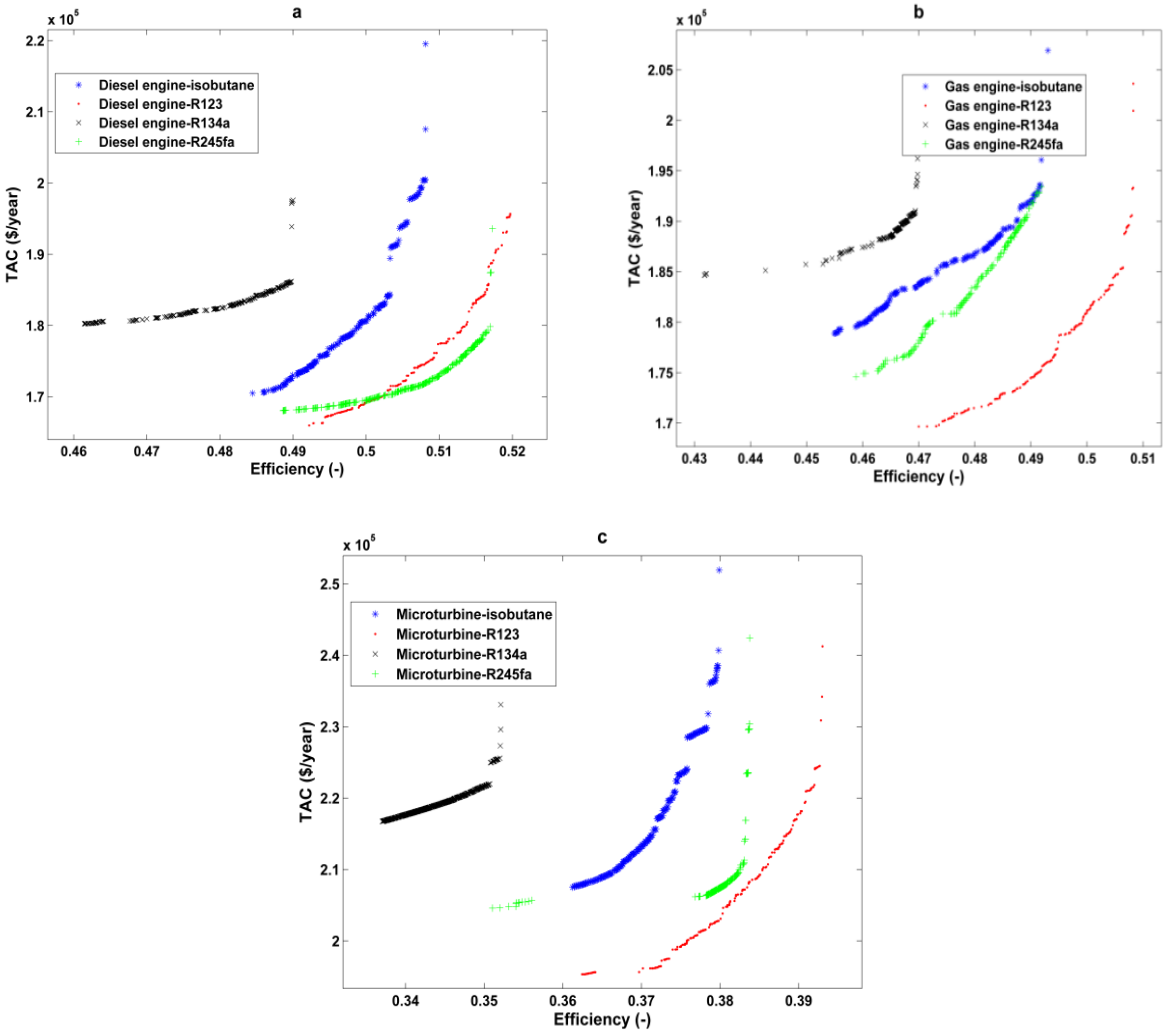

Fig. 3. Pareto front in different working fluids. a. Diesel engine, b. Gas engine, c. Microturbine

The Pareto-optimal fronts for various prime movers in a particular working fluid are demonstrated in Fig. 4. It is observed that the Pareto fronts of the microturbine did not dominate the other available fronts. Nevertheless, the worst PMs from an economical and thermodynamic efficiency viewpoint for this case study was the microturbine. According to Fig. 4, the Pareto front in the case of the diesel engine dominated the other studied PMs in all the cases, including isobutane, R123, R134a, and R245fa.

The distribution of design variables on Pareto fronts for isobutene is shown in Fig. 5. For the sake of simplicity, the distribution of design variables for the remaining studied refrigerants is not depicted. Dotted lines mark the lower and the upper limits of variables. The following results for the optimal variables distribution can be inferred as follows:

1. The refrigerant that has a higher value of efficiency needs a lower capacity prime mover (PM).
2. The prime movers operate in the range of 94–100%, 83–98%, and 99–100% of their nominal capacity for the diesel engine, gas engine, and microturbine, respectively. In fact, the PM efficiency increases for a higher PM partial load and, as a result, the PM power increases while the available heat decreases. Consequently, the PM power increases while the ORC power decreases with an increase of the PM partial load.
3. The refrigerant with a higher critical temperature will have a lower turbine inlet and condenser pressure.
4. The efficiency increases with a decrease in condenser pressure, but it is limited by the constraint presented in Eq. (28). As a

result, a refrigerant with a higher critical temperature is more appropriate for a low condenser pressure.

5. Turbine and pump isentropic efficiency are selected at their maximum allowable range. The capital cost of the system increases with an increase in turbine and pump isentropic efficiency, but the operating cost related to the fuel decreases. A selection of maximum isentropic efficiency indicated that a decrease of operating cost dominates over the increase of capital cost.
6. The regenerator effectiveness is selected in the range of 0.05–0.49. This range of selected effectiveness indicated that a regenerator is needed, but just for those with lower effectiveness. In fact, the condenser inlet temperature decreases with an increase in regenerator effectiveness and the constraint in Eq. (28) is violated for higher regenerator effectiveness.
7. In general, there are conflicts between the objective functions in the case of the distribution design parameters. In fact, a wide range of these specific parameters could be chosen, which achieve the nondominated point on the Pareto front. In this study, the PM nominal capacity causes a conflict between the objective functions. The highest nominal capacity has the highest efficiency, but it also incurs the highest capital cost.

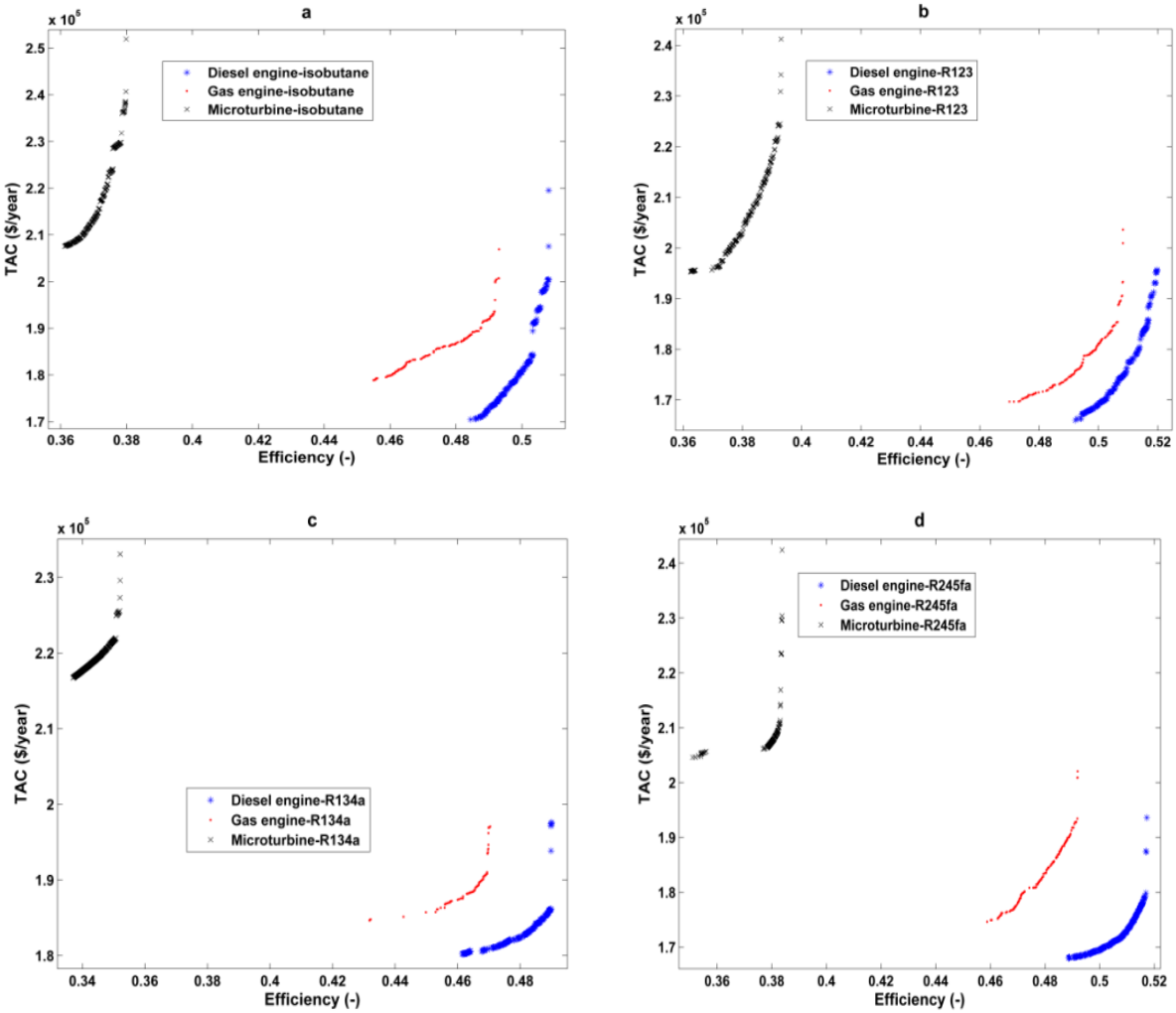

Fig. 4. Pareto front in different prime movers. a. isobutane, b. R123, c. R134a, d. R245fa

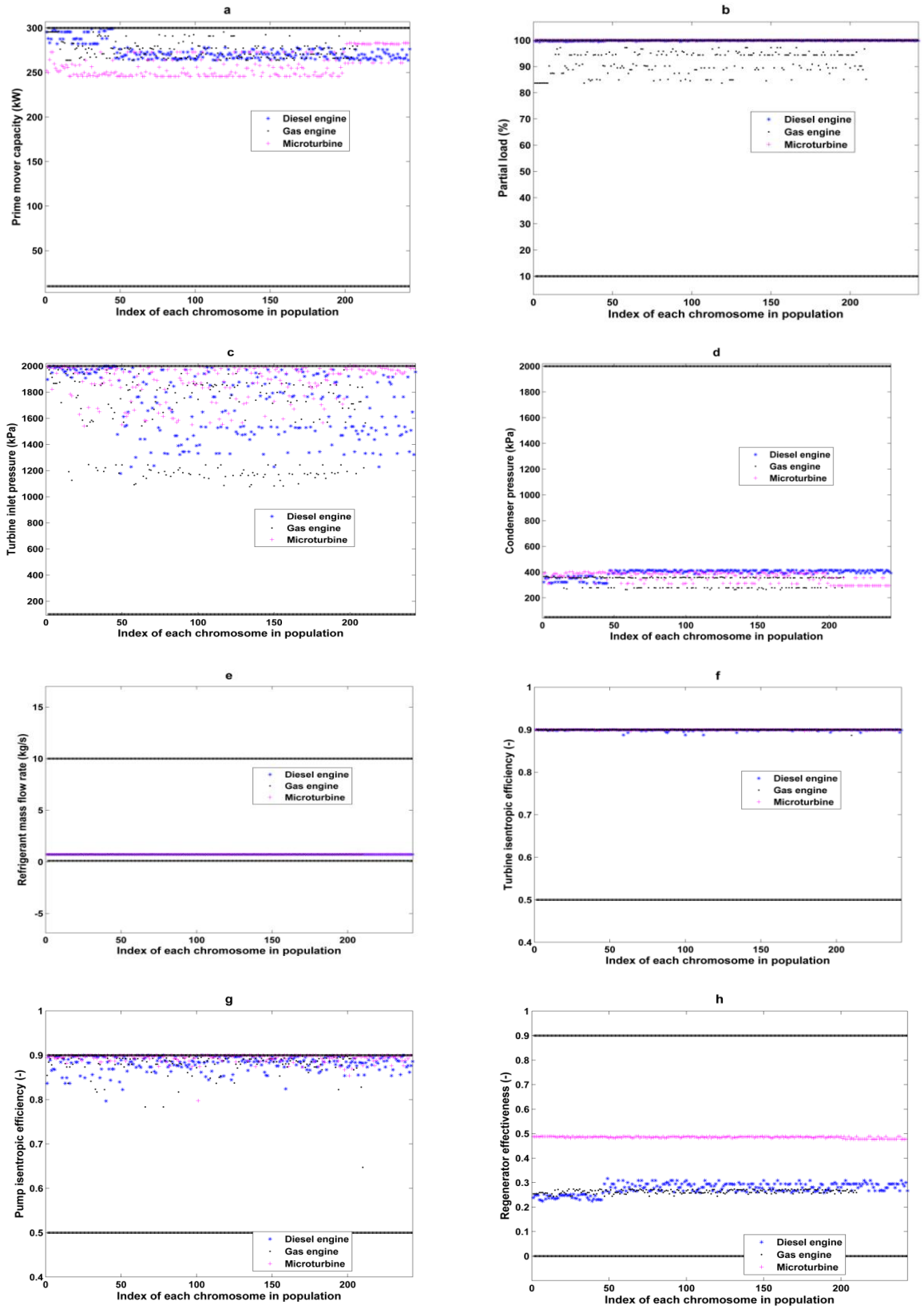

Fig. 5. Distribution of optimum values of design parameters for points in pareto front related to fluid isobutane. a. prime mover capacity, b. prime mover partial load, c. turbine inlet pressure, d. condenser pressure, e. refrigerant mass flow rate, f. turbine isentropic efficiency, g. pump isentropic efficiency, h. regenerator effectiveness

6.3. Selection of the final optimal solution

In this paper, a LINMAP (linear programming techniques for multidimensional analysis of preferences) method is used for the final optimum points [30–32]. The final value of the design parameters and the optimum objective functions for the three studied PMs (diesel engine, gas engine, and microturbine) are listed in Tables 2–4 and are discussed in the following subsections.

6.3.1. Diesel engine as a prime mover

The best refrigerant from an economical viewpoint is the diesel engine as PM and R123, which bear a total annual cost of $170,276/year. The refrigerants R245fa, isobutene, and R134a, with a total annual cost of $171,509/year, $173,845 /year, and $183,233/year, respectively, are the next in line in terms of ranking. The optimum TAC in the case of R123 is improved by 0.72%, 2.09%, and 7.60%, respectively, in comparison to R245fa, isobutene, and R134a. The refrigerant R123 is also the best refrigerant from a thermal

Table.2. The final optimum values of design parameters and objective functions for four refrigerants and diesel engine as prime mover

Case studies	Isobutane	R123	R134a	R245fa
Capacity (kW)	266.09	263.77	281.87	263.75
Partial load (%)	99.99	99.79	94.38	95.78
Turbine inlet pressure (kPa)	1507.53	802.19	1643.55	1106.84
Condenser pressure (kPa)	414.17	108.06	537.65	110.94
Refrigerant mass flow rate (kg/s)	0.71	1.33	1.22	1.03
Turbine isentropic efficiency (-)	0.90	0.90	0.90	0.90
Pump isentropic efficiency (-)	0.89	0.90	0.89	0.88
Regenerator effectiveness (-)	0.29	0.18	0.25	0.19
Thermal efficiency (-)	0.49	0.50	0.48	0.50
Total annual cost ($/year)	173,845	170,276	183,233	171,509

Table.3. The final optimum values of design parameters and objective functions for four refrigerants and gas engine as prime mover

Case studies	Isobutane	R123	R134a	R245fa
Capacity (kW)	276.21	267.79	281.87	281.89
Partial load (%)	90.17	90.68	90.85	89.45
Turbine inlet pressure (kPa)	1727.32	1025.79	1972.59	1054.42
Condenser pressure (kPa)	354.69	86.54	537.52	175.99
Refrigerant mass flow rate (kg/s)	0.72	1.33	1.33	1.33
Turbine isentropic efficiency (-)	0.90	0.90	0.90	0.89
Pump isentropic efficiency (-)	0.89	0.88	0.90	0.83
Regenerator effectiveness (-)	0.26	0.13	0.22	0.25
Thermal efficiency (-)	0.47	0.49	0.46	0.47
Total annual cost ($/year)	186,577	174,568	188,430	180,873

Table.4. The final optimum values of design parameters and objective functions for four refrigerants and microturbine as prime mover

Case studies	Isobutane	R123	R134a	R245fa
Capacity (kW)	247.37	245.62	263.75	234.29
Partial load (%)	99.99	99.96	100	99.99
Turbine inlet pressure (kPa)	1872.05	1089.55	1814.73	1677.40
Condenser pressure (kPa)	395.54	105.29	538.45	103.33
Refrigerant mass flow rate (kg/s)	0.71	1.33	1.37	1.03
Turbine isentropic efficiency (-)	0.90	0.90	0.90	0.90
Pump isentropic efficiency (-)	0.89	0.87	0.89	0.89
Regenerator effectiveness (-)	0.48	0.38	0.33	0.33
Thermal efficiency (-)	0.36	0.37	0.34	0.37
Total annual cost ($/year)	211,522	201,575	220,471	206,902

efficiency viewpoint, with a thermal efficiency of 0.50. The optimum efficiency in the case of R123 is improved by 0%, 2%, and 4%, respectively, while compared with R245fa, isobutene, and R134a.

6.3.2. Gas engine as prime mover

The best refrigerant from an economical viewpoint in the case of a gas engine as PM is R123, with a total annual cost of $174,568/year. The refrigerants R245fa, isobutene, and R134a, with total annual costs of $180,873/year, $186,577 /year, and $188,430/year, respectively, are the next in line in terms of ranking. The optimum TAC in the case of R123 is improved by 3.61%, 6.87%, and 7.94%, respectively, in comparison with R245fa, isobutene, and R134a. The refrigerant R123 is also the best refrigerant from the thermal efficiency viewpoint, with a thermal efficiency of 0.49. The optimum efficiency in the case of R123 in comparison to R245fa, isobutene, and R134a are improved by 4.08%, 4.08%, and 6.12%, respectively.

6.3.3. Microturbine as prime mover

The best refrigerant from an economical view point and in the case of a microturbine as PM is R123, with a total annual cost of $201,575/year. The refrigerants R245fa, isobutene, and R134a, with total annual costs of $206,902/year, $211,522 /year, and $220,471/year, respectively, are the next in line in terms of ranking. The optimum TAC in the case of R123 is improved by 2.64%, 4.93%, and 9.37% in comparison with R245fa, isobutene, and R134a, respectively. The refrigerant R123 is also the best refrigerant from a thermal efficiency viewpoint, with a thermal efficiency of 0.37. The optimum efficiency in the case of R123 is improved by 0%, 2.70%, and 8.10% in comparison to R245fa, isobutene, and R134a, respectively.

Therefore, the best-studied prime mover and refrigerant from the thermo-economical viewpoint is the diesel engine and R123, with a total annual cost of $170,276/year and a thermal efficiency of 0.50. In addition, a plant with the refrigerant R123 in each prime mover needs the lowest prime mover capacity, turbine inlet pressure, and condenser pressure in comparison to plants with other studied refrigerants.

7. Conclusion

In this work, the multiobjective optimization of a regenerative ORC system with different prime movers, including a diesel engine, a gas engine, and a microturbine, was studied. The nominal capacity of the prime mover, prime mover operating partial load, turbine inlet pressure, condenser pressure, refrigerant mass flow rate, turbine isentropic efficiency, pump isentropic efficiency, and regenerator effectiveness were selected as the decision variables. The efficiency and the total annual cost were considered as the two objective functions and optimization was performed for four working fluids: isobutane, R123, R134a, and R245fa. The following conclusions can be deduced from the studies on a system:

1. The diesel engine as a PM and ORC with R123 as the working fluid has the best thermo-economic results in comparison to the PMs of other studies and refrigerants.
2. R123 is the best working fluid in the all studied PMs and is followed by R245fa, isobutene, and R134a.
3. The optimum result of a diesel engine with R123 improved the efficiency by 2%, 6%, and 26% in comparison to a gas engine with R123, a gas engine with R245fa, and a microturbine with R245fa, respectively. The above percentages were 2.52%, 6.22%, and 21.50% for TAC.
4. The working fluid with a higher critical temperature leads to a lower value of turbine and condenser inlet pressure for each PM.
5. The refrigerants with the highest critical temperature and the lowest critical pressure have the best thermo-economic and environment results.
6. A regenerator improved the thermo-economic results for the all studied PMs and refrigerants. Generally, a regenerator with the low effectiveness is required.

References

[1] Mago P. J., Exergetic Evaluation of an Organic Rankine Cycle Using Medium-Grade Waste Heat, Energy Sources, Part A, Recovery, Utilization, and Environmental Effects (2012) 34(19): 1768-1780.

[2] Carcasci, Carlo, Riccardo Ferraro, and Edoardo Miliotti, Thermodynamic Analysis of an Organic Rankine Cycle for Waste Heat Recovery from Gas Turbines, Energy (2014) 65: 91-100.

[3] Yun E., Park H., Yoon S.Y., Kim K.C., Dual Parallel Organic Rankine Cycle (ORC) System for High Efficiency Waste Heat

Recovery in Marine Application, Journal of Mechanical Science and Technology (2015)29(6): 2509-2515.

[4] Gong X. W., Wang X. Q., Li Y. R., Wu C. M., Thermodynamic Performance Analysis of a Coupled Transcritical and Subcritical Organic Rankine Cycle System for Waste Heat Recovery, Journal of Mechanical Science and Technology (2015) 29(7): 3017-3029.

[5] Coskun A., Ali B., Mehmet K., Thermodynamic Analysis and Optimization of Various Power Cycles for a Geothermal Resource, Energy Sources, Part A, Recovery, Utilization, and Environmental Effects (2016) 38(6): 850-856.

[6] Li Y.R., Mei-Tang D., Chun-Mei W., Shuang-Ying W., Chao L., Potential of Organic Rankine Cycle Using Zeotropic Mixtures as Working Fluids for Waste Heat Recovery, Energy (2014) 77: 509-519.

[7] Umesh K., Karimi M.N., Asjad M., Parametric Optimisation of the Organic Rankine Cycle for Power Generation from Low-Grade Waste Heat, International Journal of Sustainable Energy (2016) 35(8): 774-792.

[8] Rahbar K., Saad M., Raya K. A., Moazami N., Modelling and Optimization of Organic Rankine Cycle Based on a Small-Scale Radial Inflow Turbine, Energy Conversion and Management (2015) 91: 186-198.

[9] Roy J. P., Mishra M. K., Ashok M., Parametric Optimization and Performance Analysis of a Regenerative Organic Rankine Cycle Using Low–Grade Waste Heat for Power Generation, International Journal of Green Energy (2011) 8(2): 173-196.

[10] Hajabdollahi Z., Hajabdollahi F., Tehrani M., Hajabdollahi H., Thermo-Economic Environmental Optimization of Organic Rankine Cycle for Diesel Waste Heat Recovery, Energy (2013) 63: 142-151.

[11] Yang M.H., Rong-Hua Y., Thermo-economic Optimization of an Organic Rankine Cycle System for Large Marine Diesel Engine Waste Heat Recovery, Energy (2015) 82: 256-268.

[12] Yang M.H., Rong-Hua Y., Analyzing the Optimization of an Organic Rankine Cycle System for Recovering Waste Heat from a Large Marine Engine Containing a Cooling Water System, Energy Conversion and Management (2014) 88: 999-1010.

[13] Michel F., Kheiri A., Pelloux-Prayer S., Performance Optimization of Low-Temperature Power Generation by Supercritical ORCs (Organic Rankine Cycles) Using Low GWP (Global Warming Potential) Working Fluids, Energy (2014) 67: 513-526.

[14] Yang M.H., Rong-Hua Y., Thermodynamic and Economic Performances Optimization of an Organic Rankine Cycle System Utilizing Exhaust Gas of a Large Marine Diesel Engine, Applied Energy (2015) 149: 1-12.

[15] Yongqiang F.,, Zhang Y., Li B., Yang J., Shi Y., Comparison between Regenerative Organic Rankine Cycle (RORC) and Basic Organic Rankine Cycle (BORC) Based on Thermoeconomic Multi-Objective Optimization Considering Exergy Efficiency and Levelized Energy Cost (LEC), Energy Conversion and Management (2015) 96: 58-71.

[16] Spayde E., Pedro J. M., Evaluation of a Solar-Powered Organic Rankine Cycle Using Dry Organic Working Fluids, Cogent Engineering (2015) 2(1): 1085300.

[17] Salcedo R., Antipova E., Boer D., Jiménez L., Guillén-Gosálbez G., Multi-Objective Optimization of Solar Rankine Cycles Coupled with Reverse Osmosis Desalination Considering Economic and Life Cycle Environmental Concerns, Desalination (2012) 286: 358-371.

[18] Boyaghchi A. F., Heidarnejad P., Thermoeconomic Assessment and Multi Objective Optimization of a Solar Micro CCHP Based on Organic Rankine Cycle for Domestic Application, Energy Conversion and Management (2015) 97: 224-234.

[19] Hajabdollahi H., Ganjehkaviri A., Nazri Mohd Jaafar M.. Thermo-Economic Optimization of RSORC (Regenerative Solar Organic Rankine cycle) Considering Hourly Analysis, Energy (2015).

[20] Imran M., Muhammad U., Byung-Sik P., Hyouck-Ju K., Dong-Hyun L., Multi-Objective Optimization of Evaporator of Organic Rankine Cycle (ORC) for Low Temperature Geothermal Heat Source, Applied Thermal Engineering (2015) 80: 1-9.

[21] Walraven D., Ben L., William D., Economic System Optimization of Air-Cooled Organic Rankine Cycles Powered by Low-Temperature Geothermal Heat Sources, Energy (2015) 80: 104-113.

[22] El-Wakil M.M. Powerplant Technology, McGraw-Hill (2002).

[23] ASHRAE Handbook Cogeneration Systems and Engine and Turbine Drives (1999).
[24] Srinivas N., Deb K., Multiobjective Optimization Using Nondominated Sorting in Genetic Algorithms, Journal of Evolutionary Computing (1994) 2(3): 221–248.
[25] Deb K., Goel T., Controlled Elitist Non-Dominated Sorting Genetic Algorithms for Better Convergence, in Proceedings of The First International Conference on Evolutionary Multi-Criterion Optimization, Zurich (2001)385–399.
[26] Deb K., Multi-Objective Optimization Using Evolutionary Algorithms, John Wiley and Sons, Chichester, UK (2001).
[27] Hajabdollahi F., Hajabdollahi Z., Hajabdollahi H., Soft Computing Based Multi-Objective Optimization of Steam Cycle Power Plant Using NSGA-II and ANN, Applied Soft Computing (2012): 12(11): 3648-3655.
[28] www.ifco.org, [Web Site of Iranian Fuel Conservation Organization].
[29] Xu J., Yu C., Critical Temperature Criterion for Selection of Working Fluids for Subcritical Pressure Organic Rankine Cycles, Energy (2014)74: 719-733.
[30] Branke J., Miettinen K., Slowinski R., Multiobjective Optimization, Interactive and Evolutionary Approaches, Springer (2008) 5252.
[31] Khorasani Nejad E., Hajabdollahi F., Hajabdollahi Z., Hajabdollahi H., Thermo-Economic Optimization of Gas Turbine Power Plant with Details in Intercooler, Heat Transfer-Asian Research (2013) 42 (8): 704-723.
[32] Mokhtari H., Esmaieli A., Hajabdollahi H., Thermo-Economic Analysis and Multiobjective Optimization of Dual Pressure Combined Cycle Power Plant with Supplementary Firing, Heat Transfer-Asian Research (2016)45(1):59-84.

Appendixes

Appendix A. Recoverable heat from the prime movers (kW) [23]

Prime mover	Recoverable heat
Diesel engine	$\frac{\dot{Q}_{DE}}{\dot{m}_{f,DE}\ LHV_{f,D}} = \frac{24.01\exp(-0.0248\ PL)+15.35\exp(0.002822\ PL)+0.001016\ PL^2-0.1423\ PL+31.72)}{100-15\ \dot{m}_{f,DE}\ Cp(T_{stack}-T_{amb})}$
Gas engine	$\frac{\dot{Q}_{GE}}{\dot{m}_{f,GE}\ LHV_{f,g}} = \frac{17.49\exp(-0.07512\ PL)+39.36\exp(-0.002556\ PL)+8.566\exp(-0.02619\ PL)+18.91\exp(0.001194\ PL)}{100-15\ \dot{m}_{f,GE}\ Cp(T_{stack}-T_{amb})}$
Microturbine	$\frac{\dot{Q}_{M}}{\dot{m}_{f,M}\ LHV_{f,g}} = \frac{24.01\exp(-.0248\ PL)+15.35\exp(0.002822\ PL)+0.001016\ PL^2-0.1423\ PL+31.72}{100-15\ \dot{m}_{f,M}\ Cp(T_{stack}-T_{amb})}$

Appendix B. Power generation by prime movers (kW) [23]

Prime mover	Power
Diesel engine	$\frac{\dot{W}_{DE}}{\dot{m}_{f,DE}LHV_{f,D}} = 1.07\exp(-0.0005736\ PL)-1.259\exp(-0.05367\ PL)\ \eta_{DE,nom}$
Gas engine	$\frac{\dot{W}_{GE}}{\dot{m}_{f,GE}\ LHV_{f,g}} = (-0.0001591\ PL^2+0.024\ PL+0.1904)\ \eta_{GE,nom}$
Microturbine	$\frac{\dot{W}_{M}}{\dot{m}_{f,M}\ LHV_{f,g}} = 0.01(-0.002551\ PL^2+1.135\ PL+11.71)\ \eta_{M,nom}$

Appendix C. Fuel consumption of prime movers (kg/s) [23]

Prime mover	Fuel mass flow
Diesel engine	$\frac{\dot{m}_{f,DE}}{\dot{m}_{f,nom}} = -0.02836\exp(0.03254\ PL)+0.2556\exp(0.01912\ PL)$
Gas engine	$\frac{\dot{m}_{f,GE}}{\dot{m}_{f,nom}} = 0.2408\exp(0.01403\ PL)+0.03553\exp(-0.02494\ PL)$
Microturbine	$\frac{\dot{m}_{f,M}}{\dot{m}_{f,nom}} = 0.4772\exp(0.007565\ PL)-0.2123\exp(-0.02677\ PL)$

Appendix D. Nominal efficiency of prime movers (-) [23]

Prime mover	Nominal capacity
Diesel engine	$\eta_{DE,nom} = \frac{1.2(0.0007973E_{nom,PM}+35.26)}{100}$
Gas engine	$\eta_{GE,nom} = \frac{1.22(0.0007973E_{nom,PM}+30.75)}{100}$
Microturbine	$\eta_{M,nom} = \frac{1.6(-9.209\times10^{-8}\ E_{nom,PM}^2+0.001724E_{nom,PM}+18.1)}{100}$

Appendix E. Purchase equipment cost functions ($) [23 and 27]

Components	Investment cost
Turbine	$C_{inv,T} = 3880.5P_{i,T}^{0.7}\left(1+\left(\frac{0.05}{1-\eta_T}\right)^3\right)\times\left(1+5exp\left(\frac{T_{i,T}-592.85}{10.42}\right)\right)$
Pump	$C_{inv,Pump} = 705.48\times\frac{1+0.2}{1-\eta_{Pump}}P_{o,Pump}^{0.71}$
Condenser	$C_{inv,cond} = 150A_{cond}^{0.8}$
Regenerator	$C_{inv,R} = 90A_R^{0.6}$
Diesel engine	$C_{PM,DE} = \left(0.9\times\left(-99.65E_{nom,PM}^{0.3324}+3446\right)\right)E_{nom,PM}$
Gas engine	$C_{PM,GE} = \left(-99.65E_{nom,PM}^{0.3324}+3446\right)E_{nom,PM}$
Microturbine	$C_{PM,M} = \left(1.212\times10^4E_{nom,PM}^{-0.03799}-6387\right)Enom_{PM}$